AAS 20-695

GEOMETRICAL TOOLS FOR THE SYSTEMATIC DESIGN OF LOW-ENERGY TRANSFERS IN THE EARTH-MOON-SUN SYSTEM

Anastasia Tselousova[*], Maksim Shirobokov[†], and Sergey Trofimov[‡]

Weak stability boundary (WSB) trajectories are Sun-perturbed low-energy trajectories connecting a near-Earth orbit and a lunar orbit. Among their benefits are the increased mass delivered to a working orbit and larger launch windows. However, the flight is much longer than for traditional high-energy lunar transfers. Since the discovery of WSB trajectories several decades ago, they have been being designed numerically, by a single or multiple shooting procedure. The major challenge is in choosing a good initial guess for that procedure: a WSB trajectory consists of legs with alternating fast/slow dynamics and is extremely sensitive. The paper presents several geometrical tools that enable the systematic design of a high-quality initial guess in the framework of the planar bicircular four-body problem. The constraints on the launch energy C_3 and the selenocentric distance of the lunar orbit insertion point are satisfied by construction. The initial-guess planar WSB trajectory is then fed to the standard multiple shooting procedure in order to get a three-dimensional trajectory with the trans-lunar injection from a specific parking orbit adapted to the realistic ephemeris model. The technique developed is ideologically similar to the patched conic approximation for high-energy trajectories: the region of prevalence concept introduced by R. Castelli is exploited instead of the sphere of influence, so that a WSB trajectory appears to be divided into the three legs: departing, exterior, and arriving. The exterior leg, calculated in the planar four-body model, should be smoothly patched with the departing and arriving legs designed in the Earth-Moon three-body system. Numerical results for the problem of low-energy transfer to the Lunar Gateway resonant near-rectilinear halo orbit show that the adaptation to the ephemeris model is regular and straightforward, with no ad hoc intermediate steps.

INTRODUCTION

Studies of the Moon and its vicinity are of great interest for space science and space exploration. In the recent years all the world's major space agencies are jointly involved in the development of a habitable lunar orbital station called the Lunar Orbital Platform-Gateway (LOP-G).[1] The station is planned to be used as a communication hub, science laboratory, short-term habitation module and holding area for rovers and other robots. Thereby, the implementation of fuel-efficient transfers from the Earth to near-lunar orbits is currently one of the key issues.

The search for the Earth-Moon trajectories has been the subject of many scientific works. A significant contribution to study of the characteristics of space flights from the Earth to the Moon was made by the Soviet scientist V.A. Egorov. His work contains a fundamental research of direct flights

[*]Junior Researcher, Space Systems Dynamics Department, Keldysh Institute of Applied Mathematics, 4 Miusskaya Sq., 125047 Moscow, Russia.

[†]Researcher, Space Systems Dynamics Department, Keldysh Institute of Applied Mathematics, 4 Miusskaya Sq., 125047 Moscow, Russia.

[‡]Researcher, Space Systems Dynamics Department, Keldysh Institute of Applied Mathematics, 4 Miusskaya Sq., 125047 Moscow, Russia.

to the Moon. Egorov was the first to answer the questions on the minimum initial speed required to reach the Moon, possible free-return trajectories, and the influence of initial conditions on the characteristics of the lunar transfer trajectory.[2] These results directly found their application in the first lunar flights. The first simple trajectories to the Moon were obtained by the patched conic approximation method.[2] Such trajectories are distinguished by a short flight time (several days) and hyperbolic arrival velocities. Therefore, it requires a significant cost to insert a spacecraft into a final orbit around the Moon, and, these transfer trajectories are called high-energy trajectories.

When migrating from the patched conic approximation to the circular restricted three-body problem (CR3BP), a new class of efficient transfer trajectories—*low-energy trajectories*—emerges. The smart use of gravity of the primary and secondary celestial bodies enables considerable fuel savings compared to the traditional high-energy trajectories with the injection and final orbit insertion impulsive maneuvers. The price for this fuel efficiency is the significantly increased time of flight.

Probably the first example of a low-energy transfer trajectory in the Earth-Moon system was given by C. Conley in 1968.[3] He rigorously proved the existence of such trajectories and revealed their important property of *ballistic capture* when no insertion maneuver is required for a spacecraft to be captured by the Moon's gravity. The Keplerian energy is no longer the first integral in the CR3BP model and naturally changes sign while the spacecraft enters the near-Moon space. In 1990 E. Belbruno and J. Miller designed a low-energy trajectory with a ballistic capture for the Hiten mission.[4] The exact term *ballistic capture* seems to be coined by them in early 1990s.[5] In contrast to capture by executing a LOI impulse, ballistic capture is temporary. It is also referred to as weak. Later, V.V. Ivashkin presented some results of analysis of effects produced by solar and terrestrial perturbations on the motion of a spacecraft in the Earth-Moon-Sun system, which is useful for a better understanding of the mechanism of capture by the Moon.[6]

Several scientists, following Conley's ideas, have developed numerical methods for constructing low-energy trajectories based on the CR3BP dynamical system characteristics. The general idea of these methods involves a search for heteroclinic transfers between the invariant manifolds of periodic or quasiperiodic orbits around libration points.[7–10] To study the properties of low-energy trajectories in the three-body (Earth-Moon) and four-body (Earth-Moon-Sun) systems, Belbruno extended the sphere of influence concept and introduced the concept of *weak stability boundary* (WSB).[5] The initial algorithmic definition of WSB as a boundary of the region in the configuration space where the orbital motion around one of the bodies is stable, was later reformulated in terms of the dynamical systems theory: the weak stability boundary for a given body is a set in the phase space that lies in the intersection of a certain Jacobi integral manifold and the region bounded by the hypersurface of zero Keplerian energy.[11,12] In the planar CR3BP, using the tools of Poincaré map and Keplerian map, the researchers revealed chaotic nature of the ballistic capture phenomenon and its intrinsic link with the WSB and resonant orbits. The resonance hopping theory has then been developed[11–16] and geometric evidence have been discovered indicating the close connection between the WSB set and hyperbolic invariant manifolds of libration point orbits.[17,18]

Among the practical achievements attributed to the WSB theory, two missions stand out: aforementioned Japanese Hiten (1990) and NASA's GRAIL (2011). In both missions, to design a trajectory ended with lunar ballistic capture, the algorithmic WSB definition was exploited. Furthermore, the solar gravitational perturbation played the key role in both cases: low-energy trajectories first depart far away from the Earth-Moon system, where the Sun's gravity pulls the perigee. After that, a spacecraft heads toward the Moon to be captured ballistically. This type of low-energy trajectories is now commonly referred to as the WSB transfer. An extensive global search of optimal two-impulse Earth-to-Moon transfers in the planar bicircular restricted four-body problem (BR4BP) clearly demonstrates that it is WSB-type trajectories that have maximum fuel efficiency, especially if a lunar fly-by is included.[19]

To this moment, all the existing techniques of designing a WSB trajectory rely on direct numerical optimization procedures, usually of shooting type. The aim of this research is to develop geometrical and analytical tools that enable the systematic design of WSB trajectories with specified parameters in some simplified dynamical model. A designed WSB trajectory should be usable as an initial guess in the multiple-shooting algorithm adjusting it to the high-precision ephemeris model of motion and given launch conditions. For simplicity, the initial approximation is constructed in planar models. The major obstacle to regular convergence of the shooting procedure from a not-so-good approximation is due to departure and arriving trajectory legs in the fast dynamics near-Earth and near-Moon regions, which causes high sensitivity to boundary conditions. The same issue for high-energy trajectories is successfully resolved by the patched conic approximation decoupling the design of a sensitive trajectory leg in the vicinity of the fly-by body. The idea put forward in this study is somewhat similar: it is based on the concept of the *region of prevalence* recently introduced by R. Castelli.[20] Following Castelli, the boundary of the Earth-Moon region of prevalence consists of points in the configuration space where the error in the right-hand side of the spacecraft's equations of motion would have the same magnitude independently of what body we neglect in the Earth-Moon-Sun system—the Moon or the Sun. So that, we divide a WSB trajectory into the three legs: arriving and departing, calculated in the planar Earth-Moon CR3BP, and exterior one, designed in the Earth-Moon-Sun planar BR4BP. These legs then should be smoothly patched on the boundary of the region of prevalence. For convenience, we replace the departing leg with an Earth collision trajectory of a required launch energy C_3. Furthermore, while patching the exterior and arriving legs, the transit trajectories (passing inside the Moon's Hill sphere) are targeted, i.e. such trajectories that belong to the interior of the two-dimensional tube generated by stable manifold trajectories of the planar Lyapunov orbit with the corresponding Jacobi integral level.

The structure of the paper is as follows. First, we outline the CR3BP and BR4BP models of motion, in which initial guess planar WSB trajectories are generated. The high-fidelity model of motion used for accurate simulation is also introduced. Second, the systematic planar WSB trajectory design is provided in detail, including the definition of the Earth-Moon region of prevalence and WSB trajectory construction on each of the three segments: departing, exterior and arriving. We also explicitly prove the second/fourth quarter rule, a well-known property of a lunar WSB transfer. Finally, to illustrate the adaptation of planar WSB trajectories to the realistic high fidelity model of motion, we calculate the WSB transfer from the Baikonur launch parking orbit ($h = 200$ km, $i = 51.6$ deg) to the L_2 southern near-rectilinear halo orbit (NRHO) 9:2, the primary candidate for the nominal orbit in the ongoing LOP-G project. The conclusion section contains the summary of the research.

DYNAMICAL MODELS

Circular restricted three-body problem

The circular restricted three-body problem models the motion of the spacecraft of negligible mass under the gravitational field of two primaries, the Earth and the Moon in our case, that are revolving with constant angular velocity in circular orbits around their center of mass C. We denote by m_E and m_M the masses of the Earth and the Moon, respectively. The equations of motion of the CR3BP are usually written in the standard rotating coordinate frame (see Figure 1) with the origin at C;

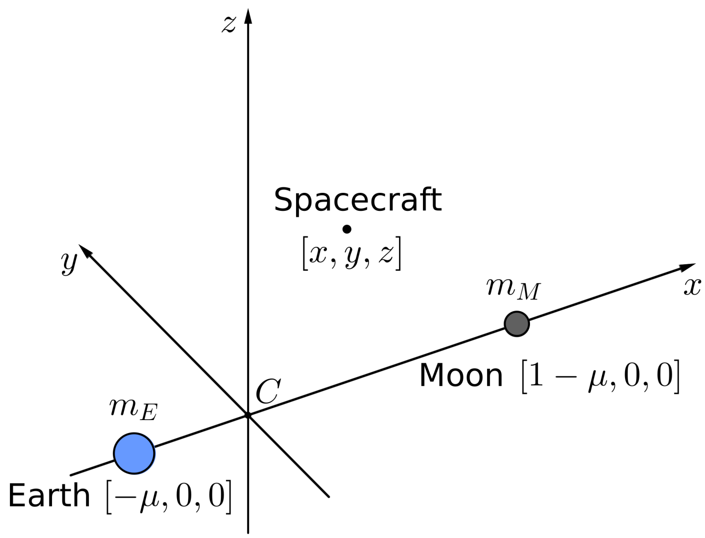

Figure 1. Rotating reference frame in the Earth-Moon circular restricted three-body problem.

the x-axis connects the masses m_E and m_M towards m_M, the z-axis is directed along the angular velocity of the orbital motion of m_M around m_E, and the y-axis completes the right-handed system.

It is also convenient to use a dimensionless system of units in which $1)$ masses are normalized so that $m_E = 1 - \mu$ and $m_M = \mu$ where $\mu = m_M/(m_E + m_M)$, $2)$ the angular velocity of the rotating frame is normalized to one, and $3)$ the distance between m_E and m_M is normalized to one. Thus, the dimensionless universal gravitational constant G is also identically equal to one. For the Earth-Moon system, corresponding units of distance, velocity and time are the following:

$$\begin{aligned} \text{DU} &= 384402 \text{ km}, \\ \text{VU} &= 1.024544182251307 \text{ km/s}, \\ \text{TU} &= 4.342513772754916 \text{ days}, \end{aligned}$$

and the mass parameter $\mu = 0.012150584460351$. In this system of units, m_E and m_M are at fixed positions along the x-axis at $[-\mu, 0, 0]$ and $[1 - \mu, 0, 0]$, respectively. The equations of motion are expressed in the nondimensional form as

$$\begin{aligned} \ddot{x} - 2\dot{y} &= \frac{\partial \Omega_3}{\partial x}, \\ \ddot{y} + 2\dot{x} &= \frac{\partial \Omega_3}{\partial y}, \\ \ddot{z} &= \frac{\partial \Omega_3}{\partial z} \end{aligned} \tag{1}$$

where

$$\Omega_3(x, y, z) = \frac{x^2 + y^2}{2} + \frac{1-\mu}{r_1} + \frac{\mu}{r_2} + \frac{\mu(1-\mu)}{2}$$

is the effective potential. The distances to m_E and m_M are given by the equalities

$$r_1^2 = (x + \mu)^2 + y^2 + z^2,$$

$$r_2^2 = (x - 1 + \mu)^2 + y^2 + z^2.$$

The system (1) has an integral of motion, the Jacobi integral,

$$J(x, y, z, \dot{x}, \dot{y}, \dot{z}) = 2\Omega_3(x, y, z) - (\dot{x}^2 + \dot{y}^2 + \dot{z}^2),$$

and, thus, a solution lies on the manifold $\mathcal{J}(J_{EM}) = \{[x, y, z, \dot{x}, \dot{y}, \dot{z}] \in \mathbb{R}^6 | J(x, y, z, \dot{x}, \dot{y}, \dot{z}) = = J_{EM}\}$ for some energy level J_{EM}. A planar motion can be obtained by setting $z \equiv 0$.

Bicircular restricted four-body problem

The bicircular restricted four-body problem incorporates the perturbation of the third primary. When constructing Earth-Moon WSB transfers, the gravitational perturbations from the Sun play a key role. Thus, in this context, it is reasonable to consider the Earth-Moon-Sun BR4BP. The Sun is assumed to revolve in a circular orbit of radius $L \gg 1$ around the Earth-Moon center of mass in the same plane (see Figure 2). The direction to the Sun in the CR3BP rotating reference frame is

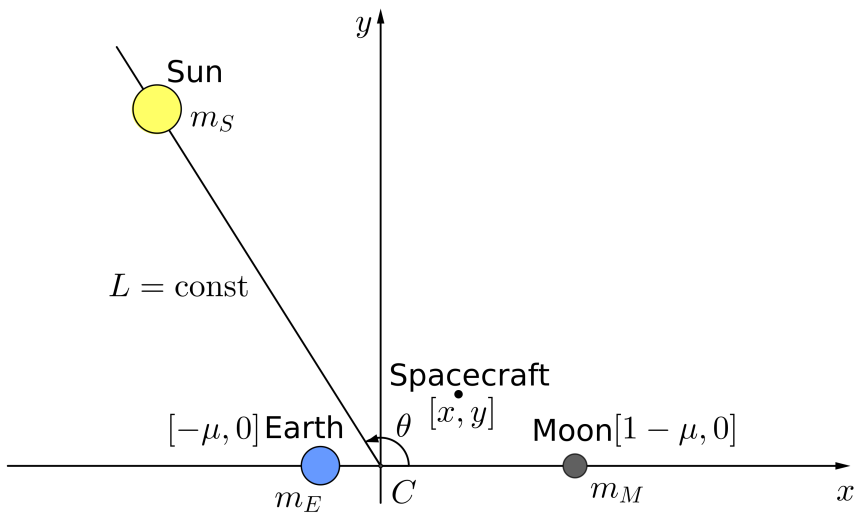

Figure 2. Rotating reference frame in the Earth-Moon-Sun planar bicircular four-body problem.

determined by θ — the phase of the Sun.

In order to obtain the BR4BP equations of motion in the nondimentional form from the CR3BP ones, it is enough to replace the effective potential by

$$\Omega_4(x, y, z) = \Omega_3(x, y, z) + \Omega_{4b}(x, y, z, t) = \Omega_3(x, y, z) + \frac{Gm_S}{r_3(t)} - \frac{Gm_S}{L^2}(x \cos\theta(t) + y \sin\theta(t))$$

where $r_3(t) = \sqrt{(x - L\cos\theta(t))^2 + (y - L\sin\theta(t))^2 + z^2}$ is the distance from the spacecraft to the Sun, $Gm_S = 3.289005596145305 \times 10^5$ is the dimensionless gravitational parameter of the Sun, and the phase of the Sun linearly grows over time: $\theta(t) = \theta_0 + w_S(t - t_0)$. For $L = 389.17$, that corresponds to 1 a.u., the orbital velocity of the Sun is determined as follows:

$$w_S = \sqrt{\frac{1 + m_S}{L^3}} - 1 \approx -0.9253.$$

By analogy with the CR3BP, a planar case is obtained when $z \equiv 0$.

High-fidelity model of orbital motion

In addition to the CR3BP and the BR4BP models, the ephemeris model is used to provide high accuracy when simulating real missions. The high-fidelity model of motion includes the central gravitational fields of the Earth and the Moon, gravitational perturbations from the Sun and all the planets of the Solar system, as well as solar radiation pressure. The lunar gravitational acceleration $\mathbf{g}_m$ is evaluated based on the spherical harmonic model GRGM1200A* truncated to degree and order 8, when the motion of the Solar system's celestial bodies, as well as the orientation of the lunar principal axes of inertia relative to the axes of the International Celestial Reference System (ICRS) are determined from JPL's DE430 ephemeris.[21]

When dealing with the equations of spacecraft motion, it is convenient to move the origin of the reference frame from the barycenter of the Solar System to the Earth's center of mass. An Earth-centered system with the axes parallel to that of the ICRS axes is called the Geocentric Celestial Reference System (GCRS). Thus, the equations of motion are as follows:

$$\dot{\mathbf{r}} = \mathbf{g}_m - \delta\varkappa^2 \frac{PA}{m}\frac{\mathbf{r}_s - \mathbf{r}}{|\mathbf{r}_s - \mathbf{r}|^3} + \frac{\mu_s}{|\mathbf{r}_s - \mathbf{r}|^3}(\mathbf{r}_s - \mathbf{r}) - \frac{\mu_s}{|\mathbf{r}_s|^3}\mathbf{r}_s + \sum_{k=1}^{8}\left(\frac{\mu_k}{|\mathbf{r}_k - \mathbf{r}|^3}(\mathbf{r}_k - \mathbf{r}) - \frac{\mu_k}{|\mathbf{r}_k|^3}\mathbf{r}_k\right),$$

where the indices m, s and k relate to the Moon, the Sun, and the kth planet, respectively. To simulate the solar radiation pressure force, the cannonball model with the spacecraft's area-to-mass ratio 0.006 m^2/kg is used. The coefficient $\delta \in [0; 1]$ represents the level of illumination, and the constant $P = 4.56 \cdot 10^{-6}$ Pa can be interpreted as solar radiation pressure at $\varkappa = 1$ a.u. distance from the Sun. The gravitational parameters of all the celestial bodies μ_s and μ_k, $k = \overline{1, 8}$ are taken from the Astronomical Almanac 2018. †

CONSTRUCTION OF PLANAR WSB TRAJECTORIES

Regions of prevalence

The BR4BP model represents the main geometrical and energy properties of WSB trajectories and, at the same time, is fairly simple. Nevertheless, even this simple model can be further simplified by first considering the planar case and than using the idea of dividing space into regions where one of the systems, Earth-Moon or Sun-Earth, prevails. This idea of space decomposition into *regions of prevalence*, similarly to the principle underlying the patched conic approximation model, was recently proposed by R. Castelli.[20] He defined the boundary of the Earth-Moon region of prevalence as points in the configuration space where the error in the right-hand side of the spacecraft's equations of motion would have the same magnitude independently of what body we neglect in the Earth-Moon-Sun system—the Moon or the Sun. Thereby, in the context of the three-body problem models, the Earth-Moon CR3BP is appropriate model to describe the dynamics inside the region of prevalence, while outside this region, the gravitational field of the Sun is predominant over the Moon's one, and the Sun-Earth CR3BP model is better to use.

In the planar BR4BP model, the region of prevalence is time-dependent and parameterized by the solar phase angle θ. The boundaries of the Earth-Moon region of prevalence, depending on θ, are shown by colored closed curves in Figure 3. For our purposes, we introduce the mean-square averaged region of prevalence having an elliptical boundary with the main axes parallel to

*https://pgda.gsfc.nasa.gov/products/50
†http://asa.usno.navy.mil/

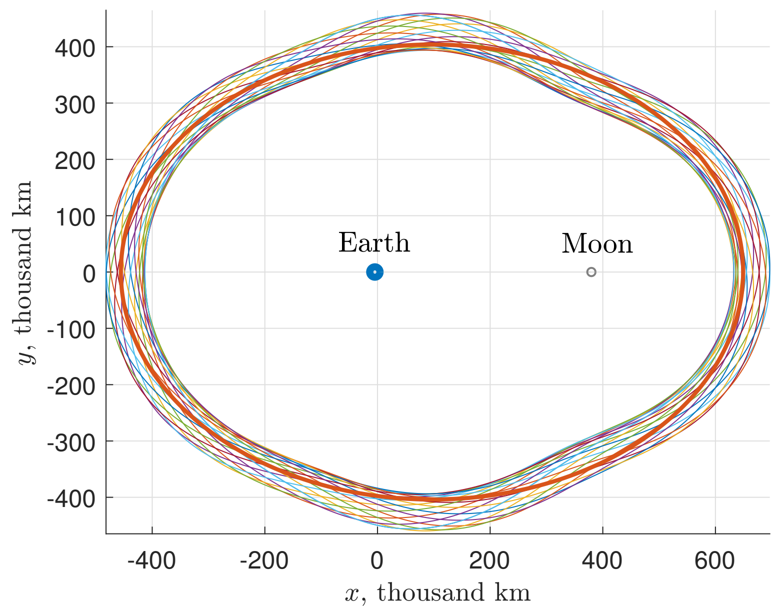

Figure 3. Earth-Moon region of prevalence boundaries for different Sun phase angles and the orange elliptical boundary of the mean-square averaged region of prevalence.

the coordinate axes of the Earth-Moon reference frame. This stationary boundary is represented in Figure 3 by a solid orange line.

Further, to construct planar WSB trajectories, we use the Earth-Moon CR3BP model everywhere inside the Earth-Moon region of prevalence, and the BR4BP model — outside it.

Synthesis of arriving legs with specified parameters

In the planar Earth-Moon CR3BP, the 3D manifold of the constant Jacobi integral level J_{EM} is divided into two non-overlapping parts by the stable invariant manifold of the planar Lyapunov orbit with the same value of J_{EM}. Thus, for a planar low-energy trajectory to be transit (i.e., passing inside the lunar Hill sphere), it should belongs to the interior of the stable manifold tube with the corresponding Jacobi integral level (see Figure 4).

In the x–$\dot{x}$ plane, the manifold trajectories, when crossing the Earth-Moon region of prevalence boundary, form a closed curve limiting the L_2 lunar gateway (Figure 5). Let P denote a set of inner points of the gateway. Note that for any point of P and a given $[x_P, \dot{x}_P]$, the corresponding coordinate y_P may be found from the condition of belonging to the region of prevalence boundary, while $\dot{y}_P$ is determined by the energy relation $J(x_P, y_P, \dot{x}_P, \dot{y}_P) = J_{EM}$. The propagation of the initial condition $[x_P, y_P, \dot{x}_P, \dot{y}_P]$ in the CR3BP will give a trajectory passing inside the Hill sphere of the Moon.

Each point of P produces a trajectory with a certain value of the perilune distance r_p and the argument of the perilune ω_p (in the planar case, the angle between the Cx axis of the Earth-Moon rotating reference frame and the direction to the perilune). It is convenient to display initial data for the trajectories with a given value of r_p and/or ω_p on the lunar gateway in the form of gradient-colored contour lines. Figure 6 shows the line $r_p = 3141$ km on the L_2 gateway with $J_{EM} = 3.06$.

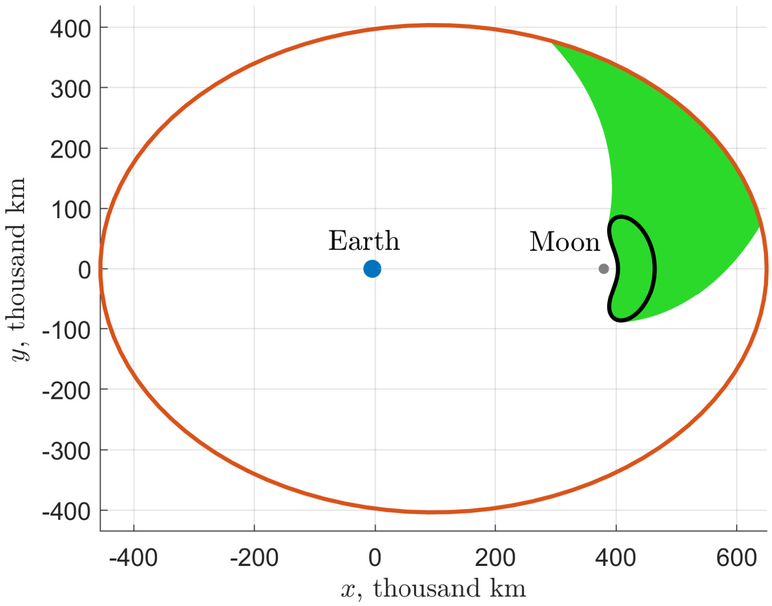

Figure 4. The stable manifold of the $J_{EM} = 3.06$ planar Lyapunov orbit propagated backward till the intersection with the boundary of the mean-square averaged Earth-Moon region of prevalence. On the 3D Jacobi integral hypersurface in the four-dimensional phase space, the transit trajectories belong to the interior of the 2D stable manifold tube.

Such values of the Jacobi integral and perilune distance coincide with the values for the NRHO 9:2. The color of the contour line points indicates the ω_p value of the approaching trajectory. Consequently, to obtain the arriving leg with specified r_p and ω_p values, the corresponding point of P should be targeted when the exterior leg of a WSB trajectory is designed. However, not all points are equally convenient for WSB trajectories to pass through. At the initial stage of designing a planar WSB transfer, it is recommended to target an arbitrary point of the gateway.

Note that the L_2 lunar gateway collapses to a point when $J_{EM} \approx 3.18$. It means that transfers to lunar orbits with $J_{EM} > 3.18$ are not possible without performing the lunar orbit insertion (LOI) maneuver. For almost Keplerian orbits around the Moon, the Jacobi integral can be estimated using the approximate formula $J_{EM} \approx 3 + W_z - 2E$, where W_z is the z-component of the orbital momentum of a spacecraft, and E is the Keplerian energy in the spacecraft-Moon two-body system. In the planar case, this expression can be rewritten in terms of the distance to the perilune r_p and perilune velocity v_p as follows:

$$J_{EM} = 3 + r_p v_p - v_p^2 + \frac{2\mu}{r_p}.$$

At the same time, the required LOI impulse at the perilune of the arriving trajectory is estimated as a solution of the quadratic equation $\Delta J_{EM} \approx \Delta v^2 + 2v\Delta v$. It is preferable to target points of the gateways with the values of the Jacobi integral in the range $3.05 - 3.15$: the higher the value is, the lower the LOI impulse is required. However, for values that are too close to the gateway closing threshold $J_{EM} \approx 3.18$, getting the entire WSB trajectory may become problematic.

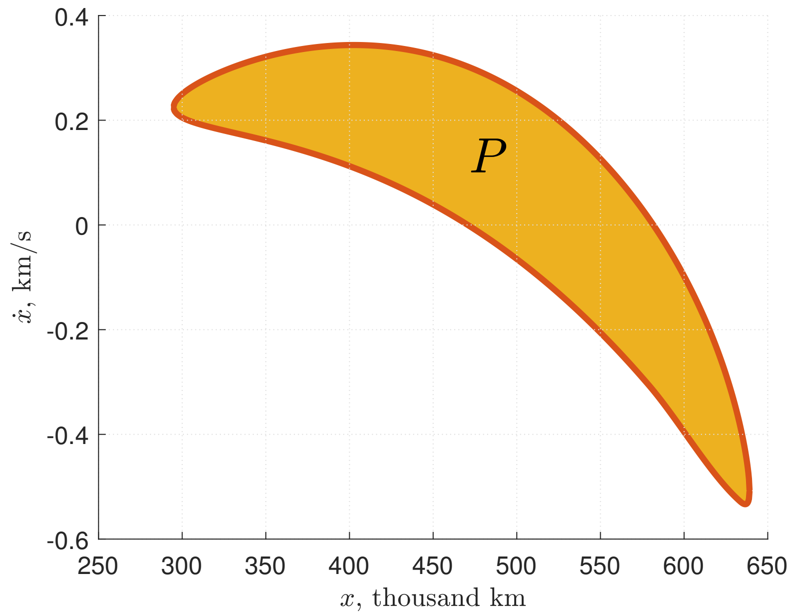

Figure 5. Lunar L_2-gateway P on the $(x, \dot{x})$ plane.

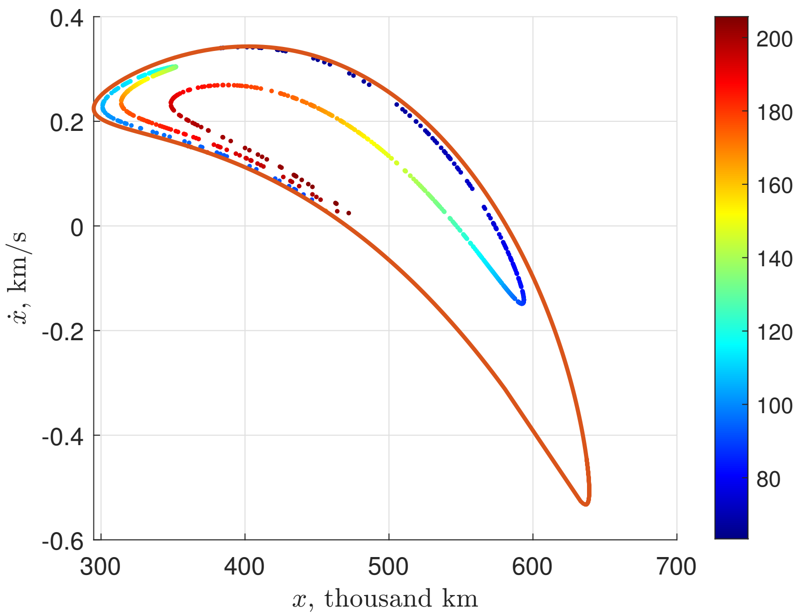

Figure 6. L_2 lunar gateway for $J_{EM} = 3.06$ (orange closed curve) and the perilune altitude contour line corresponding to the NRHO 9:2 perilune altitude value 1403 km. The color of contour line points indicates the argument of perilune (the angle between the Earth-Moon line and the direction to the perilune of a transit trajectory).

Earth collision trajectories

The departing leg of a WSB trajectory belongs to the interior of the Earth-Moon region of prevalence and it is reasonable to design this leg in the Earth-Moon CR3BP model. To simplify further analysis and avoid dependancy on a specific near-Earth orbit where Trans-Lunar Injection (TLI) departing maneuver is applied, we also propose to use collision trajectories that pass through the center of the Earth. Subsequently, such a WSB trajectory will be numerically adapted so that it starts on a desired near-Earth orbit.

When using Earth collision trajectories, it is necessary to eliminate the singularity of the CR3BP equations of motion at the point $[-\mu, 0]$. This can be achieved in a standard way by applying the Levi-Chivita transformation and transition to a new independent variable — fictitious time. The main idea of the transformation involves the following conformal mapping

$$x + \mu + iy = (u + iv)^2, i^2 = -1$$

of the plane (x, y) onto the plane of new variables (u, v). As a new independent variable, we choose the fictitious time τ associated with the physical time by the relation $dt = rd\tau$. Simple calculations give the following formulas for the change of coordinates and velocities:

$$x + \mu = u^2 - v^2,\ y = 2uv,\ \dot{x} = \frac{2(uu' - vv')}{u^2 + v^2},\ \dot{y} = \frac{2(uu' + vv')}{u^2 + v^2}.$$

Here $(.)'$ denotes the fictitious time derivative. On the plane (u, v), the center of the Earth has coordinates $u = v = 0$. The equations of motion in Levi-Chivita variables

$$\begin{aligned} u'' &= \frac{f_1(u, v)}{4} + 2(u^2 + v^2)v', \\ v'' &= \frac{f_2(u, v)}{4} - 2(u^2 + v^2)u' \end{aligned} \tag{2}$$

have no singularity at this point. In Eq. (2), the following notation is introduced:

$$\begin{aligned} f_1(u, v) = {} & \left[3(u^2 + v^2)^2 + \mu - J_{EM}\right] u - 4u^3\mu + \\ & + \frac{2\mu u}{|(u + iv)^2 - 1|} - \frac{2\mu(u^2 + v^2)(u^2 + v^2 - 1)u}{|(u + iv)^2 - 1|^3}, \end{aligned}$$

$$\begin{aligned} f_2(u, v) = {} & \left[3(u^2 + v^2)^2 + \mu - J_{EM}\right] v + 4v^2\mu + \\ & + \frac{2\mu v}{|(u + iv)^2 - 1|} - \frac{2\mu(u^2 + v^2)(u^2 + v^2 + 1)v}{|(u + iv)^2 - 1|^3}. \end{aligned}$$

Along a collision trajectory, the Jacobi integral J_{EM} is approximately equal to twice the Keplerian energy E of the spacecraft (relative to the Earth) taken with the opposite sign. At the point $u = v = 0$, the expression $J_{EM} = -2E$ becomes exact and we get

$$u'^2 + v'^2 = \frac{1 - \mu}{2}.$$

Therefore, for a given J_{EM}, the spacecraft velocity at the point $u = v = 0$ can be parametrized with one angle $\varphi \in [0; 2\pi]$:

$$u' = \sqrt{\frac{1 - \mu}{2}} \cos\varphi,\ v' = \sqrt{\frac{1 - \mu}{2}} \sin\varphi.$$

Thus, any collision trajectory depends on only two parameters: an ejection angle φ and a Jacobi constant J_{EM}, which appears in Eq. (2).

Figure 7 shows a family of the Earth collision trajectories with $J_{EM} = 0.6$ inside the region

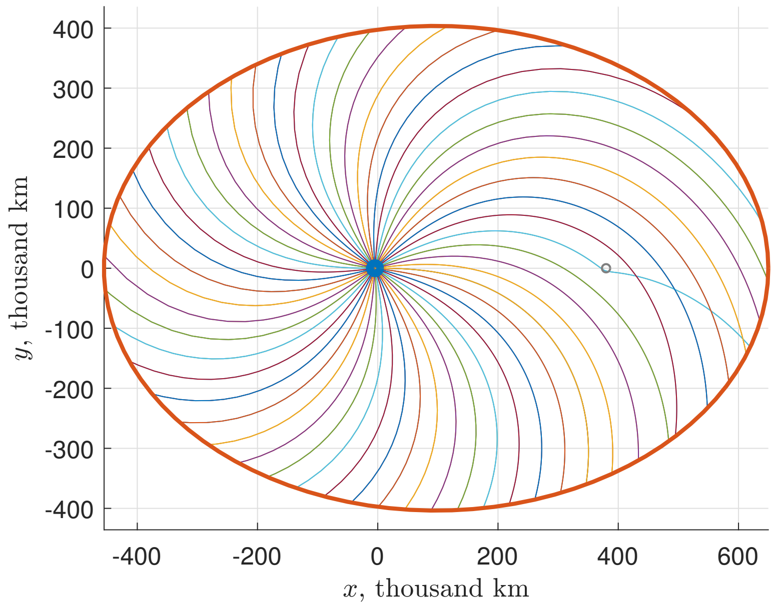

Figure 7. A bunch of Earth collision trajectories with $J_{EM} = 0.6$ (the launch energy $C_3 \approx -0.63$ km^2/s^2) propagated until they cross the region of prevalence boundary. One of the trajectories includes a lunar fly-by.

of prevalence of the Earth-Moon system. Note that in this one-parameter family of Earth collision trajectories, there exist trajectories including a lunar fly-by. Instead of the Jacobi constant, the so called characteristic energy $C_3 = -J_{EM} = 2E$ is often used. For $J_{EM} = 0.6$, we have $C_3 = -0.6$ or, in dimensional units, $C_3 = -0.63$ km^2/s^2.

Solar Gravity Effect on the Jacobi integral of the Earth-Moon system

The Sun's gravity is a key ingredient in WSB transfers. An analysis of the change in the Jacobi integral of the Earth-Moon system due to the Sun gravitational perturbation provides an insight into the geometry of WSB trajectories outside the region of prevalence of the Earth-Moon system. Taking into account the equations of motion of a spacecraft in the planar BR4BP, the change in the Jacobi integral along a certain trajectory is represented as

$$\Delta J_{EM} = -2\Delta\Omega_{4b} + 2\int \frac{\partial\Omega_{4b}}{\partial\theta}\omega_s dt \tag{3}$$

where $\omega_s = d\theta/dt$ is the constant angular velocity of the Sun in the Earth-Moon rotating frame. It is convenient to write the Sun effective potential Ω_{4b} and its derivative $\partial\Omega_{4b}/dt$ in the $Cx'y'$ coordinate system (see Figure 8) with the x-axis directed along the line connecting the Sun and the barycenter of the Earth-Moon system and then to use polar coordinates $x' = r\cos\alpha$, $y' = r\sin\alpha$. Taking into account that $r/L \ll 1$, we obtain

$$\Omega_{4b} \approx \frac{Gm_s}{L} - \frac{1}{2}\frac{Gm_s}{L^3}r^2 + \frac{3}{2}\frac{Gm_s}{L^3}r^2\cos^2\alpha.$$

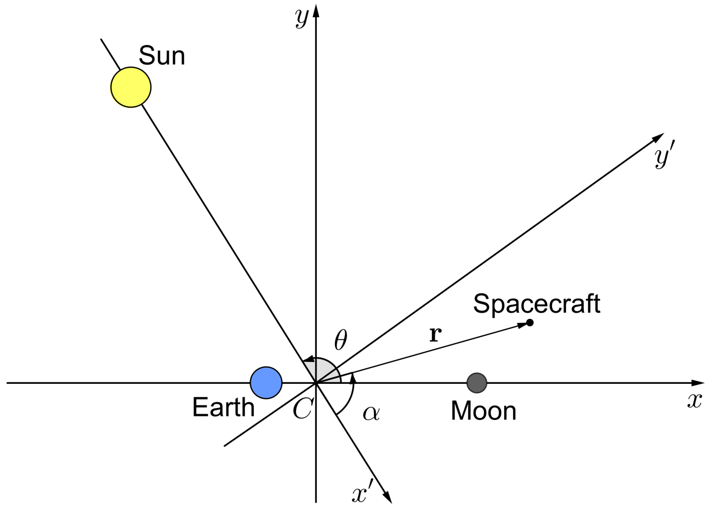

Figure 8. The Earth-Moon rotating reference frame Cxy and the Sun-barycenter of the Earth-Moon system rotating reference frame $Cx'y'$. In the Sun-barycenter coordinate system, the spacecraft radius vector is described by the polar angle α.

$$\frac{\partial \Omega_{4b}}{\partial \theta} \approx \frac{3}{2}\frac{Gm_s}{L^3} r^2 \sin 2\alpha. \tag{4}$$

For WSB trajectories, the increment of the Jacobi integral ΔJ_{EM} due to the Sun perturbation should be positive. The main contribution to this change is given by the integral term in Eq. (3). The major change occurs when the spacecraft is most distant from the Earth, more precisely, when r reaches its maximum. The positivity condition for ΔJ_{EM} at the farthest points of a WSB trajectory may be rewritten in the form $\partial \Omega_{4b}/\partial \theta < 0$. As follows from Eq. (4), this inequality is true when the apogee of the trajectory lies in the second or fourth quadrant of the $Cx'y'$ coordinate system where $\sin 2\alpha < 0$. This well-known result of the WSB theory, previously numerically discovered by many researchers, has now received an analytical explanation in the BR4BP framework and will be useful in choosing an initial approximation for the numerical algorithm of WSB trajectories patching.

Designing planar WSB transfers

We obtain a whole WSB trajectory by smoothly patching the above-mentioned three segments: the departing and arriving legs, which lie inside the Earth-Moon region of prevalence and, consequently, are modeled in the planar Earth-Moon CR3BP, with the exterior leg obtained by numerical integration in the planar BR4BP. Upon elegantly parametrizing the departing and arriving legs, the process of designing such a planar WSB trajectory is reduced to a simple optimization problem.

As optimization variables, it is convenient to choose the value of the Jacobi integral J^0_{EM}, the ejection angle φ and the phase of the Sun θ_0 at the initial epoch. On the departure segment, the equations of motion (2) are numerically integrated from the center of the Earth, i.e. with the initial condition

$$\left[0, 0, \sqrt{\frac{1-\mu}{2}}\cos\varphi, \sqrt{\frac{1-\mu}{2}}\sin\varphi\right],$$

until the intersection with the boundary of the region of prevalence. So, the values J^0_{EM} and φ uniquely define the departure leg. Then, the trajectory is propagated in the BR4BP, and the end of the external leg should target the gateway P corresponding to the desired value of the Jacobi integral J^f_{EM}. At the same time, the value of the initial Sun phase θ_0 fully defines the transition formulas between the CR3BP and the BR4BP when patching the external leg with the internal ones.

Let $\mathbf{x}_p = [x_p, y_p, \dot{x}_p, \dot{y}_p]$ be used to denote the spacecraft state vector at the boundary of the Earth-Moon region of prevalence. To get inside the lunar gateway P, it is necessary that at the point $\mathbf{x}_p$ the relation $J_{EM}(\mathbf{x}_p) = J^f_{EM}$ holds. In addition, denote with $f_1(x)$ and $f_2(x)$ the functions that define the upper and lower boundaries of the gateway in the $(x, \dot{x})$ plane (see Figure 6). They can be approximated, for example, using splines. Then, at the boundary point, the following inequalities should also be met:

$$f_1(x_p) \leq \dot{x}_p \leq f_2(x_p), \;\; x_{min} \leq x_p \leq x_{max}, \;\; y_p > 0 \tag{5}$$

where x_{min} and x_{max} are the minimum and maximum x-coordinates of the P boundary points. If the flight time is fixed, then one more constraint $t_p = t^*$ appears.

Thus, the problem of getting through the gateway P corresponding to the value of the Jacobi integral J^f_{EM} can be reduced to solving a nonlinear programming problem with the identically zero functional, the equality-type constraints

$$\begin{gathered} y_p = f(x_p), \\ J_{EM}(\mathbf{x}_p) = J^f_{EM}, \\ t_p = t^* \text{ (if required)}, \end{gathered}$$

and the inequality-type constraints (5). Here, $f(x)$ defines the boundary of the Earth-Moon region of prevalence in the coordinate space. As an initial approximation in the optimization procedure, it is convenient to take the values of J^0_{EM}, φ, and θ_0 which give a certain trajectory with an apogee in the second or fourth quadrant of the frame $Cx'y'$ and such that at time t^* it holds that $y > 0$, $x_{min} < x < x_{max}$ and the value of J_{EM} is close to J^f_{EM}.

Now let $\mathbf{x}^*_p$ be the state vector corresponding to some point of the gateway P with J^f_{EM}. As already noted, the integration of Eq. (1) from $\mathbf{x}^*_p$ provides an approach trajectory to the Moon with the specific values of r_p and ω_p. Targeting $\mathbf{x}^*_p$ adds to the set of constraints another equality-type constraints

$$\begin{gathered} x_p = x^*_p, \\ \dot{x}_p = \dot{x}^*_p. \end{gathered}$$

In this scenario the flight time is not fixed. As an initial guess, it is recommended to choose some trajectory reaching the gateway corresponding to J^f_{EM}.

The above-described exterior leg optimization problems are readily solved by MATLAB's `fmincon` solver (the *sqp* option). In the vast majority of cases, rapid convergence of the optimization process was achieved. At the output, we obtain a very good smooth initial-guess planar WSB trajectory to feed into the multiple-shooting algorithm.

Figures 9 and 10 show two examples of planar WSB trajectories corresponding to the values $J^f_{EM} = 3.06$, $r_p = 3141$ km and $\omega_p = 92°$ in the rotating Sun-Earth coordinate system centered at the center of the Earth. The departure, external, and arriving legs are drawn in green, blue, and orange, respectively. The yellow curve represents the circular orbit of the Moon.

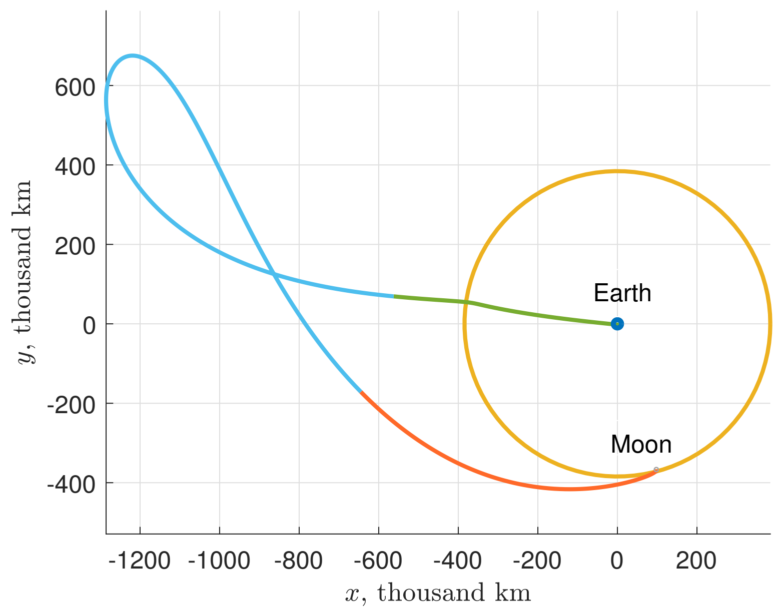

Figure 9. Initial-guess planar WSB trajectory with $J_{EM}^{0} = 1.06$, $\varphi = 14°$, $\theta_0 = 147°$, and the time of flight of 100 days.

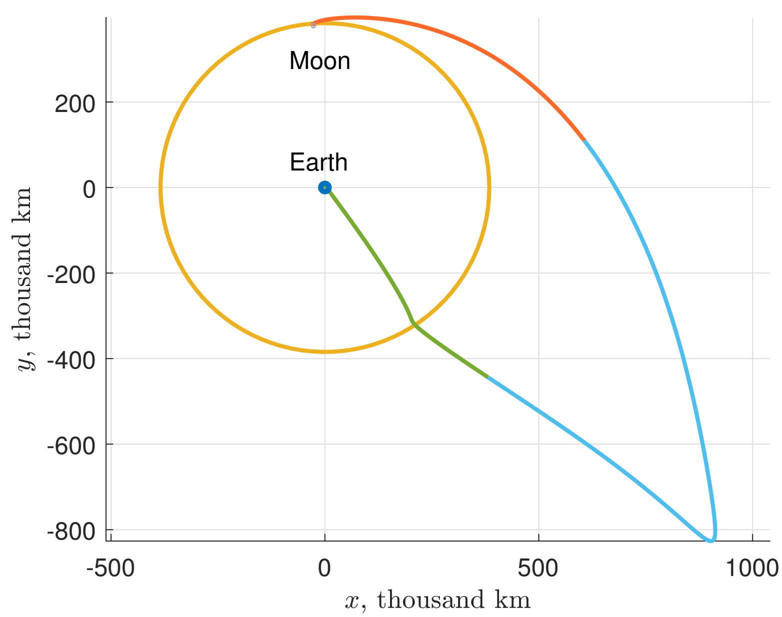

Figure 10. Initial-guess planar WSB trajectory with $J_{EM}^{0} = 1.65$, $\varphi = 199°$, $\theta_0 = 269°$, and the time of flight of 74 days.

In the first case, the optimization procedure converged to the following initial conditions: $J^0_{EM} = 1.06$, $\varphi = 14°$, $\theta_0 = 147°$. The time of flight is approximately 100 days. The second case corresponds to the initial conditions $J^0_{EM} = 1.65$, $\varphi = 199°$, $\theta_0 = 269°$; the flight time in this case is slightly less — about 74 days. Note that in both cases, the optimizer converges to a solution with an intermediate gravity assist by the Moon.

ADAPTATION OF PLANAR TRAJECTORIES TO THE EPHEMERIS MODEL AND SPECIFIC LAUNCH CONDITIONS

The adaptation of planar WSB trajectories to the high-fidelity model of motion is carried out by the multiple shooting method. The epochs and state vectors of the spacecraft in the GCRS coordinate system, as well as the LOI impulse and additional deterministic trajectory correction maneuver (TCM), were selected as the optimization variables. The initial guess for the phase variables consists of the epochs and state vectors of the spacecraft obtained in the planar case, and the initial guess for impulses can be set equal to zero. As the objective function, the sum of the squares of the TCM and LOI impulses is considered. The constraints of the multiple shooting method include requirements for

- the altitude, inclination, and eccentricity of a post-launch parking near-Earth orbit,
- the launch date and time,
- the departure impulse magnitude,
- smoothness of patching the position and velocity at all nodes of the multiple shooting method,
- conditions for entering the target orbit.

A circular 200 km orbit is taken as a low-Earth parking orbit in which a transfer to the Moon begins by applying the TLI maneuver. The parking orbit corresponds to the launch from the Baikonur cosmodrome and is fixed relative to the International Terrestrial Reference System axes: its inclination is $51.6°$, the longitude of the ascending node is $8.26°$ E. The magnitude of the TLI impulse has an upper limit of 3.2 km/s. What concerns the final lunar orbit, the L_2 southern NRHO 9:2 is assumed. We require that the final position and velocity of the spacecraft correspond to the average perilune of the NRHO orbit in the rotating Earth-Moon reference frame. The launch date is selected in accordance with the received value of θ_0 for the corresponding planar initial-guess trajectory.

A family of WSB trajectories were obtained using the multiple shooting method described above. The optimization procedure is solved using the *sqp* algorithm implemented in MATLAB's `fmincon` solver. The adaptation to the realistic ephemeris model and specific launch conditions appeared to be straightforward and relatively fast. It has been discovered that no additional intermediate steps are required for the multiple-shooting procedure to converge. After the convergence is reached, the family of WSB transfer trajectories for the whole launch window can be recovered by continuation in the launch date.

Examples of WSB trajectories from the Baikonur parking orbit to the southern NRHO 9:2 in the Earth-centered rotating Sun-Earth reference frame are shown in Figure 11. The dashed gray curve shows the initial-guess trajectory generated in the planar BR4BP. Two blue curves indicate realistic WSB trajectories corresponding to the opening and closing of the launch window characterized by the limit total cost $\Delta V_{\sum} = \Delta V_{TCM} + \Delta V_{LOI} \leq 100$ m/s. The value of the initial phase of

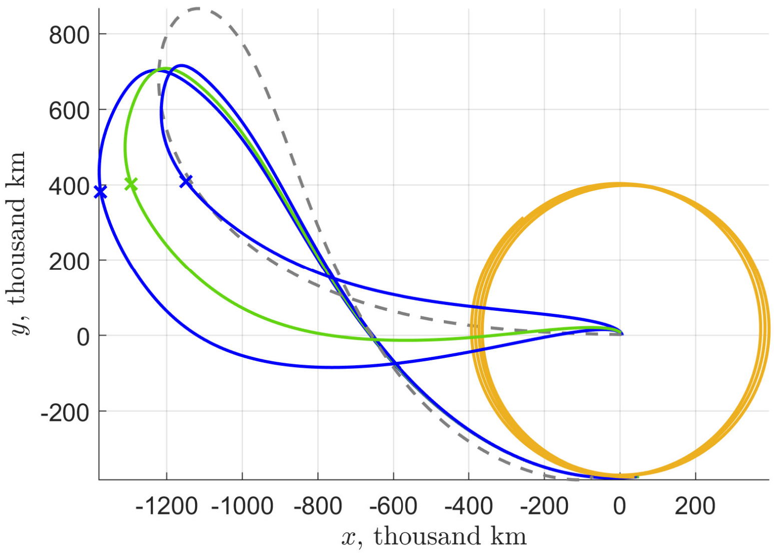

Figure 11. Initial-guess trajectory obtained in the PBR4BP (dashed gray) and realistic WSB trajectories corresponding to the opening and closing of the launch window with $\Delta V_\Sigma \leqslant 100$ m/s (both blue), as well as the optimal trajectory (green) in the Apr 2028 launch period. The 200 km, 51.6 deg parking orbit is considered. The optimal transfer with the launch date 20 Apr 2028 and the NRHO 9:2 arrival date 29 Jul 2028 demands $\Delta V_\Sigma = 10$ m/s (TCM)+67 m/s (LOI) = 77 m/s. The launch window size amounts to 14 days. Deterministic TCM points along the three realistic trajectories are indicated by crosses of respective color.

the Sun θ_0 for the initial-guess planar WSB transfer is equal to $327.5°$. Generally speaking, this value corresponds to twelve dates throughout a year; all of them can be obtained automatically. Here, the April 2028 date is selected. Thus, the first trajectory in the family was obtained for the launch date of April 27, 2028, 12:00. (For simplicity, we compute WSB trajectories discard minutes and seconds). Then, WSB trajectories with other launch dates were received by the scalar continuation method with a step of 1 hour in the start time. The arrival time is fixed: July 29, 2028, 08:13:29. Convergence from the planar initial guess took no more than 40 minutes. One step of the continuation method took approximately 10 s.

The blue trajectory with a wider loop (see Figure 11) corresponds to the launch window opening. The total impulse for this transfer is $\Delta V_{\sum} = 32.876$ m/s (TCM) $+$ 67.176 m/s (LOI) $=$ $= 100.052$ m/s. The start date is April 13, 2028, 12:00. The second blue trajectory corresponds to closing the launch window. The respective value of total cost for it is $\Delta V_{\sum} = 33.937$ m/s (TCM)$+$ $+66.096$ m/s (LOI) $= 100.034$ m/s. The TLI maneuver is performed on April 28, 2028, 04:00. Thus, the launch window size amounts to 14 days. Besides, the green trajectory indicates the fuel-optimal transfer with $\Delta V_{\sum} = 9.980$ m/s (TCM) $+$ 66.734 m/s (LOI) $= 76.714$ m/s; its launch date is April 20, 2028, 07:00. The TCM points along all the three realistic trajectories are marked by crosses.

CONCLUSION

This study presents several geometrical and analytical tools for the systematic design of planar WSB trajectories with specified characteristics in the planar BR4BP model of motion. Using the concept of the region of prevalence, a WSB trajectory is divided into the three following legs: departing, arriving, and exterior. Upon elegantly parameterizing the departing and arriving legs in the Earth-Moon planar CR3BP model, the process of designing such a planar WSB trajectory is reduced to the simple optimization problem: the exterior WSB leg, obtained by numerical integration in the planar BR4BP model, should be smoothly patched with the departing and arriving legs of given energy. Some analytical derivations have been made to help a designer in rationally choosing those energy (Jacobi integral) values. Apropos, the second/fourth quarter rule, a well-known property of a lunar WSB transfer, was proved. Following this approach, planar WSB trajectories corresponding to different launch dates and flight times have been successfully obtained.

Designed WSB trajectories represents a very good initial guess in the multiple shooting algorithm that adjusts them to the high-precision ephemeris model of motion and given launch conditions. As an example, the WSB transfer from the Baikonur launch parking orbit to the southern NRHO 9:2 was calculated for the launch date in April 2028. After that, the family of WSB transfer trajectories for the whole launch window with the total cost $\Delta V_{\sum} = \Delta V_{TCM} + \Delta V_{LOI} \leq 100$ m/s was recovered by continuation in the launch date. The launch windows size appeared to be equal to 14 days. The optimal transfer with the launch date April 20, 2028 demands $\Delta V_{\sum} = 10$ (TCM) m/s+ $+67$ (LOI) m/s $= 77$ m/s. It is worth noting that the adaptation to the high-fidelity model of motion is regular and does not require intermediate ad hoc steps, and the continuation process takes no more than a couple of iterations. Convergence from the planar initial guess took no more than 40 minutes. One step of the continuation method took approximately 10 s.

ACKNOWLEDGMENTS

The study is funded by the Russian Science Foundation (RSF), project # 19-11-00256.

REFERENCES

[1] T. Gill, "Lunar Orbital Platform-Gateway," *45th Space Congress Proceedings*, 2018, 27 p.

[2] V. A. Egorov, "On Some Problems of Dynamics for Flight to Moon," *Uspekhi Phizicheskikh Nauk*, Vol. 63, No. 1, 1957, pp. 73–117.

[3] C. C. Conley, "Low Energy Transit Orbits in the Restricted Three-Body Problem," *SIAM Journal of Applied Mathematics*, Vol. 16, No. 4, 1968, pp. 732–746.

[4] E. Belbruno and J. Miller, "A Ballistic Lunar Capture Trajectory for the Japanese Spacecraft Hiten," Tech. Rep. IOM 312/90.4-1731-EAB, JPL,California Institute of Technology, 1990.

[5] E. A. Belbruno and J. K. Miller, "Sun-Perturbed Earth-to-Moon Transfers with Ballistic Capture," *Journal of Guidance, Control, and Dynamics*, Vol. 16, No. 4, 1993, pp. 770–775.

[6] V. V. Ivashkin, "On Trajectories of Earth–Moon Flight of a Particle with Its Temporary Capture by the Moon," *Doklady Physics*, Vol. 47, No. 11, 2002, p. 825–827.

[7] K. Howell, B. Barden, R. Wilson, and M. Lo, "Trajectory Design Using a Dynamical Systems Approach With Application to Genesis," *Proceedings of the AAS/AIAA Astrodynamics Specialist Conference*, 1997.

[8] W. Koon, M. Lo, J. Marsden, and S. Ross, "Shoot the Moon," *Proceedings of the AAS/AIAA Space flight Mechanics Meeting*, 2000.

[9] G. Gomez, W. Koon, M. Lo, J. Marsden, J. Masdemont, and S. Ross, "Invariant Manifolds, the Spatial Three-Body Problem and Space Mission Design," *Proceedings of the AIAA/AAS Astrodynamics Specialist Meeting*, 2001.

[10] J. Parker and G. Born, "Modeling a Low-Energy Ballistic Lunar Transfer Using Dynamical Systems Theory," *Journal of Spacecraft and Rockets*, Vol. 45, No. 6, 2008, pp. 1269–1281.

[11] F. Topputo, E. Belbruno, and M. Gidea, “Resonant Motion, Ballistic Escape, and Their Applications in Astrodynamics,” *Advances in Space Research*, Vol. 42, No. 8, 2008, pp. 1318–1329.

[12] E. Belbruno, F. Topputo, and M. Gidea, “Resonance Transitions Associated to Weak Capture in the Restricted Three-Body Problem,” *Advances in Space Research*, Vol. 42, No. 8, 2008, pp. 1330–1351.

[13] S. D. Ross and D. J. Scheeres, “Multiple Gravity Assists, Capture, and Escape in the Restricted Three-Body Problem,” *SIAM Journal of Applied Dynamical Systems*, Vol. 6, No. 3, 2007, pp. 576–596.

[14] P. Grover and S. Ross, “Designing Trajectories in the Planet-Moon Environment Using the Controlled Keplerian Map,” *Journal of Guidance, Control, and Dynamics*, Vol. 32, No. 2, 2009, pp. 436–443.

[15] S. Campagnola and R. P. Russell, “Endgame Problem Part 2: Multibody Technique and the Tisserand-Poincaré Graph,” *Journal of Guidance, Control, and Dynamics*, Vol. 33, No. 2, 2010, pp. 476–486.

[16] G. Lantoine, R. P. Russell, and S. Campagnola, “Optimization of Low-Energy Resonant Hopping Transfers Between Planetary Moons,” *Acta Astronautica*, Vol. 68, No. 7-8, 2010, pp. 1361–1378.

[17] F. García and G. Gómez, “A Note on Weak Stability Boundaries,” *Celestial Mechanics and Dynamical Astronomy*, Vol. 97, No. 2, 2007, pp. 87–100.

[18] E. Belbruno, M. Gidea, and F. Topputo, “Weak Stability Boundary and Invariant Manifolds,” *SIAM Journal of Applied Dynamical Systems*, Vol. 9, No. 3, 2010, pp. 1061–1089.

[19] F. Topputo, “On Optimal Two-Impulse Earth-Moon Transfers in a Four-Body Model,” *Celestial Mechanics and Dynamical Astronomy*, Vol. 117, 2013, pp. 279–313.

[20] R. Castelli, “Regions of Prevalence in the Coupled Restricted Three-Body Problems Approximation,” *Communications in Nonlinear Science and Numerical Simulation*, Vol. 17, No. 2, 2012, pp. 804–816.

[21] W. M. Folkner, J. G. Williams, D. H. Boggs, R. S. Park, and P. Kuchynka, “The Planetary and Lunar Ephemerides DE430 and DE431,” *IPN Progress Report*, Vol. 42-196, 2014, 81 p.